The effect of ball milling on the structural, thermal and optical properties of TiO_2

Seema Gupta[1] and Aditya Kumar[2]

[1]Department of Physics, Kalindi college, University of Delhi, India

[2]Department of Physics and Astrophysics, University of Delhi, India

Corresponding author: seemagupta@kalindi.du.ac.in

ABSTRACT

The Titanium dioxide (TiO_2) precursors were milled for 0, 3, 6, 9 and 12 hours respectively. Size of the nanoparticles and c/a ratio is calculated using X-ray analysis and Scanning electron microscopy. The diffraction peaks for anatase and rutile phase can be observed from XRD pattern. Crystallite size is seen to be reduced as time of the milling is increased. X-ray confirms non deformation of tetragonal cubic structure for different milling time. The calculated values of dislocation density and lattice strain increase with time of milling. Differential scanning calorimetry (DSC) analysis is done in temperature range 24°C to 400°C. No phase change is observed. The number of Schottky defects as calculated remain same even after 12 hour of ball milling. UV visible shows the blue shift in absorbance curve as particle size decreases. The energy gap is increased from 3.37eV to 4.05 eV for 12hour milled sample. As sample is milled for longer time, there is reduction in particle size due to collision of balls/powder. These particles possess a higher surface to volume ratio, however result in increased dislocations and strain. As no evidence of phase change observed from both XRD and DSC, ball milling proves to be a potential method for preparing nano sized TiO_2 particles.

Key Words: Titanium dioxide, ball milling, lattice strain, dislocation density, Schottky defects, energy gap.

I. INTRODUCTION

Titanium dioxide (TiO_2) is widely researched semiconductor during the past decade due to its high chemical and physical stability (Gupta and Tripathi 2011; Testino and Bellobono 2007; Nehru et.al. 2012; Theisvanthi 2017). It is characterised by high refractive index and a wide energy gap of 3.2 eV (Gupta and Tripathi 2011). TiO_2 has been used as sensors, solar cells and against bacterial action etc (Gupta and Tripathi 2011). It is widely used as photo-catalyst for its stability, cost effectiveness and non-toxic nature (Testino and Bellobono 2007). TiO_2 exhibit three types of structures-anatase, rutile and brookite. Anatase and rutile are tetragonal, while brookite is orthorhombic. At ambient temperatures, anatase and brookite are metastable, while rutile is the most stable. However, due to low hardness, high photocatalytic activity and finer transparency, anatase form of TiO_2 is preferred in many applications (Theisvanthi 2017). Now a days TiO_2 nano particles have been synthesized using different methods- physical vapour deposition, chemical vapour deposition, hydrolysis, sol gel etc.(Pardon et.al. 2018).

Environment friendly and cost -effective nanoparticles are also prepared by egg white protein by sol gel method (Samira et.al.2013). Ball mill is a process of blending, mixing and particle size reduction which can be used to prepare small sized nano particles (Theisvanthi 2017). In ball milling process, different techniques like mechanical tumbling, mechanical alloying and mechanical milling are used for material fabrication and synthesis. The size reduction and doping of TiO_2 with different materials by ball milling method was done earlier (Theisvanthi 2017; Aravind et.al.2021). It is an eco-friendly, low cost method which can be used for large scale production of nano particles for commercial purposes. The products so obtained are chemically stable (Theisvanthi 2017).

In the current study, different sized TiO_2 nano particles are prepared by ball milling method. The effect of ball milling is studied on its structural, thermal and optical properties.

1. EXPERIMENTAL

The TiO_2 powder were purchased from Sisco research laboratories Pvt. Ltd. with purity 98%. TiO_2 appeared white in colour with a density of 4.26 g/cc and melting point is 1830^{o}C. The powder was ball milled using the planetry ball mill table top with plate RPM 200 and bowl RPM 284 for time 0, 3, 6, 9 and 12hour respectively. The structural studies were done using X-ray diffraction pattern (XRD) and scanning electron microscopy (SEM). The XRD pattern was taken using Rigaku/lambda at room temperature. Angle 2θ was varied within the range 10° to 80° with the exposure of X-rays of wavelength λ =0.15406 nm. The size of nanoparticles after 0 hour and 12 hour ball milling was also determined using SEM image taken by Jeol Scanning electron microscope. Thermal analysis for 0 hour and 12 hour ball milled samples was done by differential scanning calorimetry (DSC 2920). The machine was initially warmed up for 30 sec and then the temperature was varied from 22°C to 400°C. UV vis absorption spectrum was recorded by Motras UV-Visible true double beam spectrophotometer for 0 hour and 12 hour milled samples.

3. RESULTS AND DISCUSSION

3.1 X-RAY DIFFRACTION

The X-ray diffraction patterns for 0, 3, 6, 9 and 12 hour ball milled samples are shown in figure 1. Both anatase and rutile phase appear in the diffraction pattern. Anatase peaks are (101), (204), while rutile phase peaks are (110), (101), (100), (111), (210), (200), (211), (220), (002), (310), (300). This is in agreement with earlier reported results (Aravind et.al.2021). No phase change is observed in any of the diffraction patterns of ball milled samples. Crystallite size can be calculated by the Scherrer equation (Aravind et.al.2021)

$$D = \frac{k\lambda}{\beta \cos(\theta)} \qquad (1)$$

where D is the average size of the nano crystallite, k is Scherrer constant which is dimensionless form factor with value 0.9, β is the line broadening in radians which is determined at half the maximum intensity (FWHM).

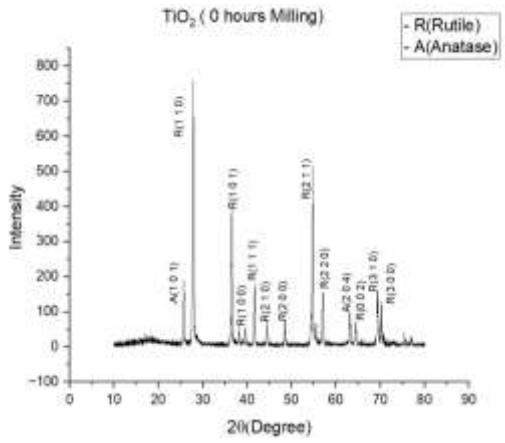

1(a)

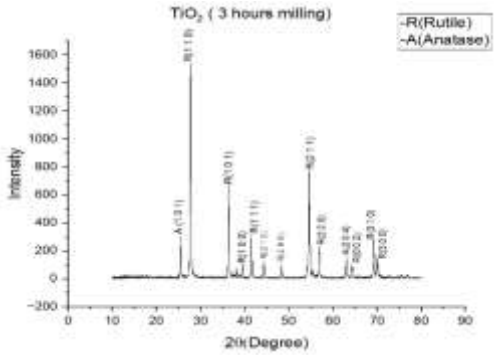

1(b)

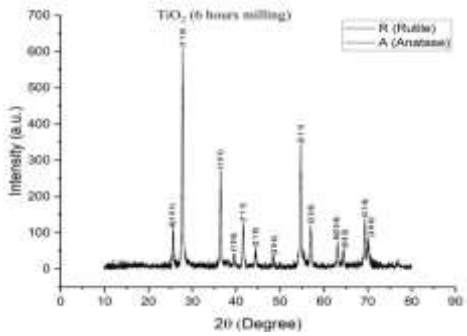

1(c)

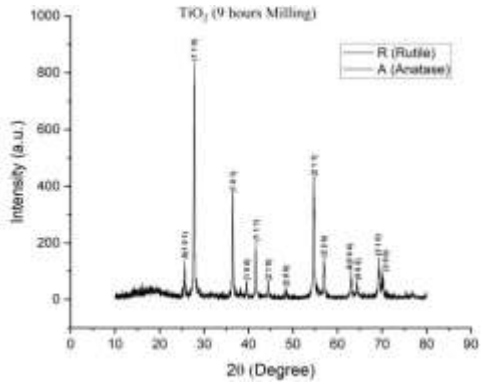

1(d)

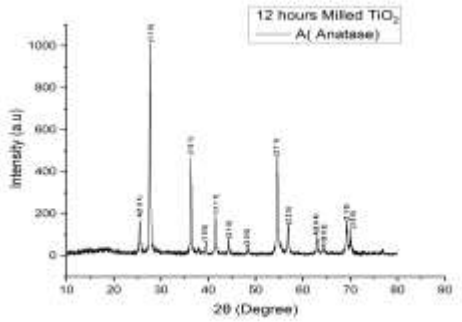

1(e)

Fig. 1: XRD pattern of (a) 0 hour, (b) 3 hour, (c) 6 hour, (d) 9 hour, (e) 12 hour ball milled samples

The calculation of lattice parameters is done using equation for interplanar spacing for tetragonal structures (Raja and Barron A.R.2022)

$$\frac{1}{d^2} = \left(\frac{h^2+k^2}{a^2} + \frac{l^2}{c^2}\right) \quad (2)$$

where d is interplanar spacing; h, k, l are miller indices; a and c are lattice constants. The interplanar spacing d is calculated using Bragg's law $2d\sin\theta = n\lambda$. The calculated values of average crystallite size and c/a ratio is shown in table 1. As the TiO_2 precursors were milled for 0,3,6,9 and 12 hours respectively, the crystallite size is seen to be reduced as time of the milling is increased (fig 2). The calculated values of c/a ratio and average size are listed in table 1. The c/a ratio calculated for anatase and rutile phase are in agreement with earlier reported results (Siddiqui 2019) and confirm the non-deformity of tetragonal structure after ball milling the sample. However, slight change observed in c/a values on ball milling is consistent with experimental results that change in lattice parameters occur with decreasing particle size (Weihong et.al.2004).

Table 1: c/a ratio and average size for TiO_2 samples with different milling time

Milling hours	Anatase c/a	Rutile c/a	Average size D(nm)
0	2.6028	0.6366	36.85
3	1.5988	0.9505	32.159
6	1.8672	0.9505	24.79
9	1.9182	0.9023	22.11
12	2.5026	0.7332	20.3

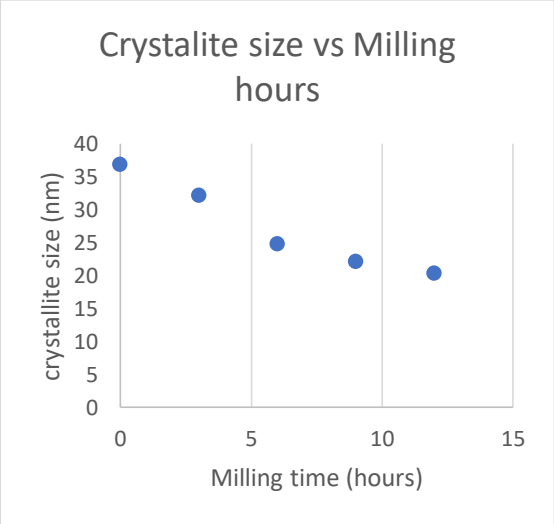

Fig 2: Variation of particle size with milling time

The lattice strain ε for 0, 3, 6, 9, 12 hour ball milled samples is estimated using Williamson-Hall equation (Theisvanthi and Alagar 2013)

$$\beta = C\,\varepsilon\,\tan\theta \qquad (3)$$

The length of dislocation lines per unit volume gives the dislocation density of the crystal (Nehru et.al 2012). The dislocation density is estimated using formula (Weihong et.al.2004)

$$\delta = 1/D^2 \qquad (4)$$

The calculated values of lattice strain and dislocation density are reported in table 2.

Table 2: The calculated values of lattice strain and dislocation density for TiO_2 samples with different milling time

Milling time	Lattice strain	Dislocation density δ $(nm)^{-2}$
0	0.00126	0.00064
3	0.00128	0.00072
6	0.00156	0.00106
9	0.00167	0.00157
12	0.00303	0.00198

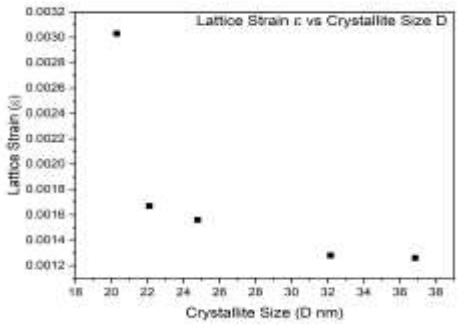

3(a)

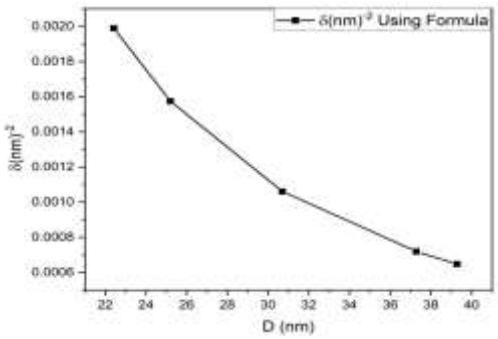

3(b)

Fig.3: Variation of (a) lattice strain and (b) dislocation density (δ) with crystallite size

Dislocation density increases with increasing milling hour. The strain is induced in the powders due to the crystal imperfections and distortion. The

calculated values of lattice strain increase as the size of crystallite decreases on increasing the time of ball milling (fig 3 a). The increase in dislocations may lead to the piling of dislocation lines against each other. This leads to their entanglement which prevents easy deformation of the grains and hence improves their hardness (Theisvanthi and Alagar 2013; Salem et.al.2023).

As the specific surface area is inversely proportional to size of the particle by relation (Theisvanthi and Alagar 2013)

$$S = 6 \times 10^3 / D\,\rho \qquad (5)$$

where ρ is the density of TiO_2, decrease in size on ball milling will lead to increased specific surface area of the particles. The morphology, crystal defects and specific surface area greatly influence photo catalytic activities of TiO_2 (Saltow and Wakamiya 2013). Although TiO_2 has limitation as photo catalysis under visible region, the increase in specific surface area with decrease in size creates more active sites for reagent molecules to get adsorbed and hence results in its enhanced photo catalytic activity (Amano et.al. 2010).

Morphology index (M.I) is estimated using formula (Theisvanthi and Alagar 2013)

$$M.I = \frac{FWHM_h}{FWHM_h + FWHMp} \qquad (6)$$

Where $FWHM_h$ is full width at half maximum for highest peak and FWHMp is full width at half maximum for a particular peak. The calculated value of M.I range from 0.78-0.61 for 0 hour sample and range from 0.46- 0.43 for 12 hour milled TiO_2 sample. The results show the uniformity and fineness of the nanoparticles ball milled for longer time.

An increase in intensity observed in diffraction peaks for 3h ball milled sample [fig. 2 b] may be due to initial improved crystallinity occurring due to ball milling. However, nonuniformity of ball milled samples may also cause variation in intensity. On further milling, the line broadening due to reduction in size and improvement of morphology leads to decrease in intensity of peaks. The decreased intensity of XRD peaks of TiO_2 with increase in duration of ball milling has been reported earlier (Sen et.al.1999; Messai et.al.2018).

3.2 Scanning electron microscopy

The SEM images of 0 hour ball milled samples and 12 hour ball milled samples are shown in figure 4.

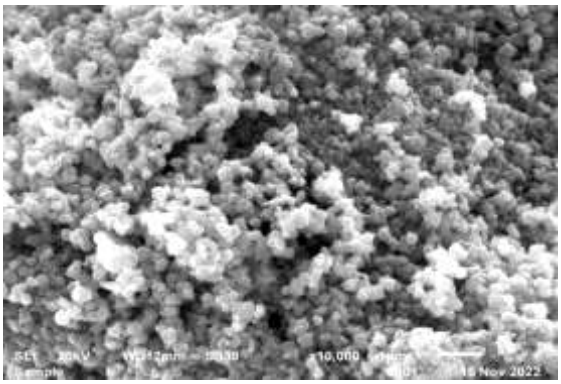

4(a)

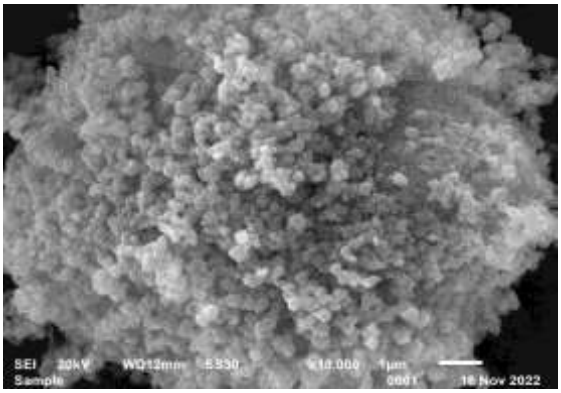

4(b)

Fig.4: SEM image of (a) 0 hour ball milled sample (b)12 hour ball milled sample

The calculated values for size are 39.47 nm for 0 hour sample and 29.81 nm for 12 hour milled sample showing the decrease in size on ball milling. However, the sizes calculated from SEM images are higher as compared from sizes calculated from XRD due to averaging.

3.3 Differential Scanning Calorimetry

DSC plots for 0 hour milled sample and 12 hour milled samples are shown in figure 5.

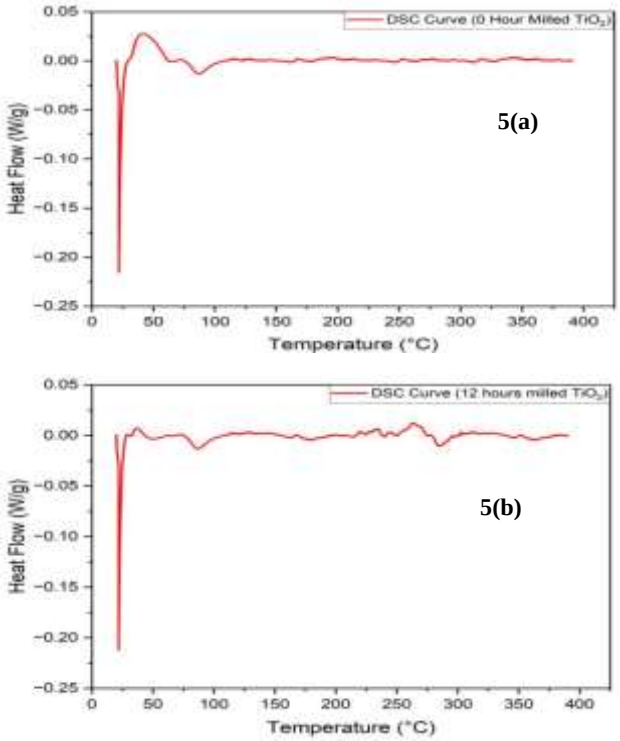

Fig.5: DSC plots of (a) 0 hour ball milled sample (b)12 hour ball milled sample

The first endothermic peak around 88°C in DSC plots of both 0 hour milled and 12 hour milled samples may be due to evaporation of weakly bounded water (Marinescu et.al 2011). However, an additional endothermic peak is observed at 285.6°C in 12hour milled sample. The high frequency, inelastic collisions during ball milling results in rise in temperature leading to loosening of chemically bound water. The decomposition of this hydroxyl group may result in an additional endothermic peak (Marinescu et.al 2011). However, no phase change is observed in the measured range of temperature.

The number of schottky defects in unit volume of crystal are calculated by (Libre Texts Chemistry 2020).

$$N_s = N \times \exp\left(-\frac{\Delta Hs}{2kT}\right) \quad (7)$$

where, N is Number of cations/anions per unit volume, T is temperature in K, ΔHs is Enthalpy for creating one schottky defect, N_S is Number of schottky defects occurs per unit volume and K is Boltzman constant.

The calculated value of $N_S = 2 \times 10^9$ which is nearly same for 0 hour and 12 hour milled samples.

3.4 *Optical Properties*

The UV-vis absorption pattern for 0 hour and 12 hour milled TiO_2 samples is shown in figure 6.

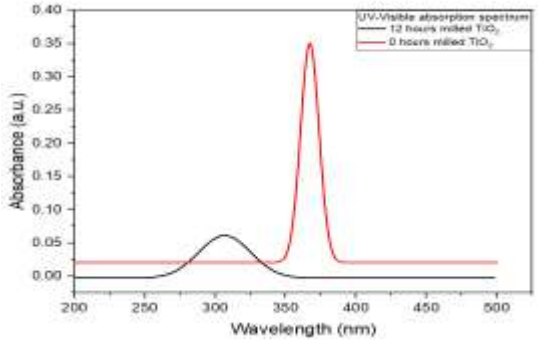

Fig. 6: UV-Visible absorbance curve for 0 hour and 12 hour milled TiO_2 samples

UV visible shows the blue shift in absorbance curve as particle size decreases for 12 hour milled sample. The energy gap is roughly estimated using the equation (Lin et.al.2006)

$E_g = h C/\lambda$ (8)

Where h is Planck's constant and C is velocity of light. The corresponding value calculated for energy gap for 0 hour milled sample is 3.37eV which is consistent with earlier reported results (Lin et.al.2006), while energy gap is 4.05eV for 12 hour milled TiO_2. The decrease in particle size decreases the overlapping of energy levels or orbitals making bands narrower. This may lead to increase in energy gap (Yadav et.al. 2012). The absorbance graphs clearly show the improved optical properties for milled sample.

4. CONCLUSION

The TiO_2 precursors were milled for 0,3,6,9 and 12 hours respectively and the crystallite size is seen to be reduced as time of the milling is increased. The c/a ratios calculated for anatase and rutile phase confirm the non-deformity of tetragonal structure. No phase change is observed in XRD pattern even after 12hour ball milling. As the milling hour are increased, the dislocation density increases indicating improvement in hardness of the sample. The lattice strain is also observed to be increasing in the samples with increase in time of ball milling. The estimated values of morphological index show uniformity and fine ness of ball milled samples. As a sample is milled for a longer time, there is a reduction in particle size due to the collision of balls/powder. These particles possess a higher surface area to volume ratio, thereby generating a number of lattice imperfections, such as dislocations and lattice strain. However, the number of Schottky defects in unit volume of crystal came out to be same after milling. UV absorption peak shows a blue shift after milling for 12 hours and improvement in optical properties. The reduction of size by ball milling method may additionally create increase in oxygen vacancies and mobility of oxygen ions. This provides materials with improved application as catalytic support (Rinaudo et.al. 2020). The increase in dislocation density and strain may provide enhanced reactivity of TiO_2 nanostructures (Chi 2020). Being environment friendly and cost effective, ball milling may be taken as a potential method to produce large scale nano particles of TiO_2 with reduced size and improved physical and optical properties.

Acknowledgement

The authors are thankful to Prof. S. Murugavel for his guidance. We wish to thank Dr. Rajesh Kumar Meena, Department of Chemistry, Kalindi college for his necessary help.

Authorship contribution statement:
Seema Gupta: Conceptualization, visualization, writing and editing, Aditya Mishra: Resources, methodology, data

References

- Amano F., Nogami K.,Tanaka M., Ohtani B.(2010). Correlation between Surface Area and Photocatalytic Activity for Acetaldehyde Decomposition over Bismuth Tungstate Particles with a Hierarchical Structure. *Langmuir*, 26(10), 7174–7180. DOI: 10.1021/la904274c.
- Aravind M., Amalanathan M., Sony M., Mary M. (2021). Synthesis of TiO_2 nanoparticles by chemical and green synthesis method and their multifaceted

properties. *Journal of applied sciences*, 3:409. DOI:10.1007/s42452-021-04281-5.

- Chi Lun Pang (2020). Strain and stress effects on single crystal supported titania and related nanostructures. *Semiconductor Science and Technolgy*, 35, 113001. DOI :10.1088/1361-6641/ab9faa.
- Gupta S.M., Tripathi M. (2011). A review of TiO_2 nanoparticles. *Chinese science bulletin*, 56(16), 1639-1657, DOI:10.1007/s 11434-011-4476-1.
- Libre Texts Chemistry (2020). Schottky defects, https://chem.libretexts.org/Bookshelves/Inorganic_Chemistry/Supplemental_Modules_and_Websites_(Inorganic_Chemistry)/Crystal_Lattices/Lattice_Defects/Schottky_Defects.
- Lin H., Huoung C.P., Li, Ni.c., Shah S.I., Tseng Y.H. (2006). Size dependency of nanocrystalline TiO_2 on its optical property and photocatalytic reactivity exemolified by 2-chlorophenol. *Applied catalyst B: Environment*, 68, 1-11, DOI: 10.1016/j.apcatb.2006.07.018.
- Marinescu C., Sofronia A., Rusti C., Piticescu R. et.al (2011). DSC investigation of nanocrystalline TiO_2 powder. *Journal of thermal analysis and calorimetry*, 103(1), 49-57. DOI: 10.1007/s10973-010-1072-6.
- Messai Y., Vileno B., Martel D., Turek P. and Mekki D.E. (2018). Milling effect on the photo-activated properties of TiO_2 nanoparticles: electronic and structural investigations. *Bull. Mater. Sci.* 41:57, 1-11 https://doi.org/10.1007/s12034-018-1572-8.
- Nehru LC, Swaminathan V, Sanjeeviraja C. (2012). Photoluminiscence studies of nanocrystalline tin oxide powder for opto electronic devices. *American Journal of material science, 2(2), 6-10*. DOI: 10.5923/j.materials.20120202.02.
- Parden N., Omobola O., Henry M., Raymond T. and Simcelile Z(2018). Synthesis methods for titanium dioxide nanoparticles: A review. TiO_2 – Material for a sustainable environment. DOI: 10.5772/intechopen.75425.
- Raja M.V. Pawan and Barron A.R. (2022), Crystal structure. *Chemistry libre texts*, https://chem.libretexts.org/Bookshelves/Analytical_Chemistry/Physical_Methods_in_Chemistry_and_Nano_Science_(Barron)/07%3A_Molecular_and_Solid_State_Structure/7.01%3A_Crystal_Structure.
- Rinaudo M.G. , Beltrán A.M. , Fe rnández M.A. , Cadús L.E. , Morales M.R. (2020). Tailoring materials by high-energy ball milling: TiO_2 mixtures for catalyst support application. *Materialstoday Chemistry*, 17, 100340. Doi:10.1016/j.mtchem.2020.100340.
- Salem M.N., Ding K., Rodel J., Fang X.(2023). Thermally enhanced dislocation density improves both hardness and fracture toughness in single crystal $SrTiO_3$. *Journal of American ceramic society*, 106(2), 1344-1355.
- Saltow K.I., Wakamiya T. (2013). 130-fold enhancement of TiO_2 photolytic activities by ball milling, *Applied Physics letters*, 103, 031916. DOI: 10.1063/1.4816058.
- Samira B., Kamayar S., Sharifah B.A.H (2013). Synthesis and characterization of anatase titanium dioxide nanoparticles using egg white solution via sol-gel method. *Composite nanoparticles*, 2013, article ID 858205,

DOI:10.1155/2013/848205.

- Sen S., Ram M.L., Roy S., Sarkar B.K. (1999). The structural transformation of anatase TiO_2 by high energy vibrational ball milling. *Journal of material research*, 14(03), 841-848. DOI: 10.1557/JMR.1999-0112.
- Siddiqui H. (2019), Modification of Physical and chemical properties of titanium dioxide (TiO_2) by ion implantation for dye sensitized solar cells. *Ion Beam*. DOI : 10.5772/intechopen.83566 .
- Testino A., Bellobono R. l. (2007). Optimizing the photocatalytic properties of hydrothermal TiO_2 by the control of phase composition and particle morphology-A systemetic approach. *Journal of American chemical society*, 129, 3564-3574, DOI: 10.1021/ja067050.
- Theisvanthi T. (2017). Review on titania nano powder processing and application. *Condensed Matter> Material science*, https://arxiv.org/abs/1704.00981.
- Theisvanthi T., Alagar M. (2013). Titanium dioxide nanoparticles -XRD analysis an insight. *Chemical Physics*. DOI: 10.48550/arXiv.1307.1091.
- Weihong Q., Wang M.P., Su Y.C. (2004). Size effect on the lattice parameters of nanoparticles. *Journal of material science letters*, 21(11), 877-878. DOI: 10.1023/A:1015778729898.
- Yadav B.C., Shukla T., Singh S.1 and. Yadav T.P.(2012). Titania Prepared by Ball Milling: Its Characterization and Application as Liquefied Petroleum Gas Sensor https://arxiv.org/ftp/arxiv/papers/1205/1205.3032.pdf.